SCIENTIFIC REPORTS

OPEN

SUBJECT AREAS:
STATISTICAL PHYSICS, THERMODYNAMICS AND NONLINEAR DYNAMICS
COMPUTATIONAL BIOLOGY AND BIOINFORMATICS
APPLIED PHYSICS
PHYSICS

Received
20 August 2012

Accepted
7 November 2012

Published
27 November 2012

Correspondence and requests for materials should be addressed to B.W. (bingbignmath@gmail.com)

Safety-Information-Driven Human Mobility Patterns with Metapopulation Epidemic Dynamics

Bing Wang[1], Lang Cao[1], Hideyuki Suzuki[1,2] & Kazuyuki Aihara[1]

[1]Institute of Industrial Science, The University of Tokyo, 4-6-1 Komaba, Meguro-ku, Tokyo 153-8505, Japan, [2]PRESTO, Japan Science and Technology Agency (JST), 4-1-8 Honcho Kawaguchi, Saitama 332-0012, Japan.

With the help of mass media, people receive information concerning the status of an infectious disease to guide their mobility. Herein, we develop a theoretical framework to investigate the safety-information-driven human mobility with metapopulation epidemic dynamics. Individuals respond to the safety information of a city by taking safe moves (passing cities with a more number of healthy individuals) or unsafe moves (passing cities with a less number of healthy individuals). Our findings show that the critical threshold depends on mobility in such a way that personal execution of safe moves unexpectedly promotes the global spread of a disease, while unsafe moves counterintuitively cause a locally, relatively small outbreak size. Our analysis underlines the role of safety consideration in the spatial spread of an infectious disease with clear implications for the model of mobility driven by individuals' benefit.

During the past few years, reaction-diffusion processes have been successfully applied to modeling the spread of an epidemic with the considerations of individuals' mobility patterns[1–21]. Since human travel is responsible for the spatial spread of human infectious diseases, understanding human movement patterns is crucial to the modeling of metapopulation epidemic spreading. Fortunately, data on human mobility collected at a global scale[22,23], such as the world-wide air-transportation network[22,24] and at a local scale, such as bank-note circulation in the United States[25,26], US commuting network data[27], and mobile-phone data[28,29] have been broadly recorded. Consequently, mathematical modeling of the impacts of recurrent mobility patterns[22,27,30] and natural human mobility patterns[31–33] on the epidemic process has been greatly explored.

In the event of an epidemic outbreak, individuals often collect information concerning the on-going status of an infectious disease and utilize it to guide their mobility patterns[34–36]. People might prefer to stay at home rather than travel if they are aware of the seriousness of the infection; if their travel plans cannot be canceled, they might prefer to bypass infectious areas and visit only those areas that appear relatively safe with a more number of healthy individuals (we call this "safe moves"). This personal consideration of safe moves may have a profound effect on the spreading process, because the status of an epidemic in a city affects individuals' choice of mobility destination, and individuals' movement to a city further affects the epidemic spread there. Therefore, the interaction of the human mobility and the spreading process is a kind of coevolution dynamical process. Given the important relevance of safe moves to the spreading process, we investigate the impact of human mobility driven by safety information on the epidemic process.

Resorting to mathematical modeling with the metapopulation approach, we consider two possible scenarios of human mobility that encompass most of real safety information situations: (i) safe moves, and (ii) unsafe moves (we will explain it later), quantified by a set of parameters. Scenario (ii) is an inverse virtual case of safe moves. Although this assumption is somehow opposite to our intuition because individuals usually take safe moves for their own benefits, it may help us comprehensively understand the impact of different kinds of human mobility on the epidemic behavior by comparing different situations. We also have to stress that the fitting of the model parameters to practical data is beyond the scope of the present work. We find that the invasion threshold (the critical population density ρ_{0c} in a nonlimited transmission pattern[4]) alters with mobility parameters caused by safety consideration. Specifically, safe moves unexpectedly promote the global spread of a disease by lowering the critical mobility rate and increasing the outbreak size; while unsafe moves counterintuitively prevent the disease spread and reduce the outbreak size. The results underline the crucial role of human mobility in the spatial spread of a human disease.

Results

Model. A susceptible-exposed-(a)symptomatic infectious-susceptible (SEIS) model is used as a framework for the study of epidemic behavior. Each individual in a subpopulation is in one of the four states: susceptible (S), exposed or latent (E), asymptomatic infectious (A), or symptomatic infectious (I). Susceptible individuals become infected by coming in contact with symptomatic or asymptomatic infectious individuals at rate β_I or β_A, respectively; they then enter the latent state, during which state individuals contract the infection but are not yet infectious. Following a latent period of ϵ^{-1}, latent individuals enter the asymptomatic or symptomatic infectious state with a probability p_a or $1 - p_a$, respectively. After a recovery period of μ^{-1}, infectious individuals recover and return to the susceptible state. The mobility rates for individuals in states *S*, *E*, *A*, and *I* are D_S, D_E, D_A, and D_I, respectively. A realistic model should incorporate the recurrent mobility into the model, since individuals are often observed to return to their origins like commuting[27] and traveling[37]. Then, the interaction of the return rate, the diffusion rate, and the safe moves will affect the spreading process. Considering the difficulty in theoretical analysis caused by the introduction of recurrent mobility and in order to clarify the fundamental effects of safe moves on the spreading process, the mobility process is simply assumed to be in a long-term and it is solely dependent on a city's safety level as our first attempt. The safety level of a city is strongly relevant with the way it is defined (see details in the Supplementary Information). For simplicity, we assume that the safety level of a city with degree k at time t is proportional to the average number of susceptible individuals contained in it, $\rho_{S,k}(t)$. In practice, people usually receive information on the number of infected people in a city. In that case, according to our model, $\rho_{S,k}(t)$ can be calculated from the relationship $\rho_{S,k}(t) = \rho_k(t) - \rho_{E,k}(t) - \rho_{I,k}(t) - \rho_{A,k}(t)$, where $\rho_k(t)$ is the average population size in a city with degree k at time t; $\rho_{E,k}(t)$, $\rho_{I,k}(t)$, and $\rho_{A,k}(t)$ are the average numbers of exposed individuals, symptomatic infectious individuals, and asymptomatic infectious individuals in a city with degree k at time t. In the following, for convenience, let $\rho_{S,k}$ denote $\rho_{S,k}(t)$ and subpopulation with k denote subpopulation with degree k.

A common intuition about mobility is that individuals usually prefer to move to a safe city in order to protect themselves from infection. Therefore, the probability that individuals travel from subpopulation k to one of the neighboring subpopulation k', $\Theta_{kk'}$, is proportional to the subpopulation k''s safety level, $\rho_{S,k'}$. A parameter γ will be used to measure the scale of the dependence on the subpopulation k''s safety level in the form of $\rho_{S,k'}^{\gamma}$. The parameter γ can generally vary with diverse human behavior, for example, $\gamma > 0$ represents the case of safe moves (safety information positively leads people to visit a safer city), i.e., the safer a city is, the higher is the probability that people visit it, see Fig. 1. $\gamma < 0$, on the other hand, corresponds to the inverse case of safe moves, i.e., the safer a city is, the lower is the probability that people visit it. The latter assumption seems to be opposite to our intuition, since individuals usually take beneficial movements rather than take risky movements, but this situation may help us comprehensively understand how different kinds of human mobility influence the epidemic behavior with a comparative analysis. Therefore, the mobility probability matrix Θ with the entry $\Theta_{kk'} \sim \rho_{S,k'}^{\gamma}$ is defined. In addition, we assume that individuals in the same dynamic state travel in the same way, e.g., all individuals in state *S* take safe (unsafe) moves with $\gamma_S > 0$ ($\gamma_S < 0$). After the appropriate normalization and incorporating all possible states of individuals in the present model, the probability that individuals in state σ move from subpopulation k to subpopulation k', $\Theta_{kk'}^{\sigma}$, is written as

$$\Theta_{kk'}^{\sigma} = \frac{\left(\rho_{S,k'}\right)^{\gamma_\sigma}}{k\sum_{k''} p(k''|k)\left(\rho_{S,k''}\right)^{\gamma_\sigma}}, \text{ for } \sigma = S, E, A, I, \qquad (1)$$

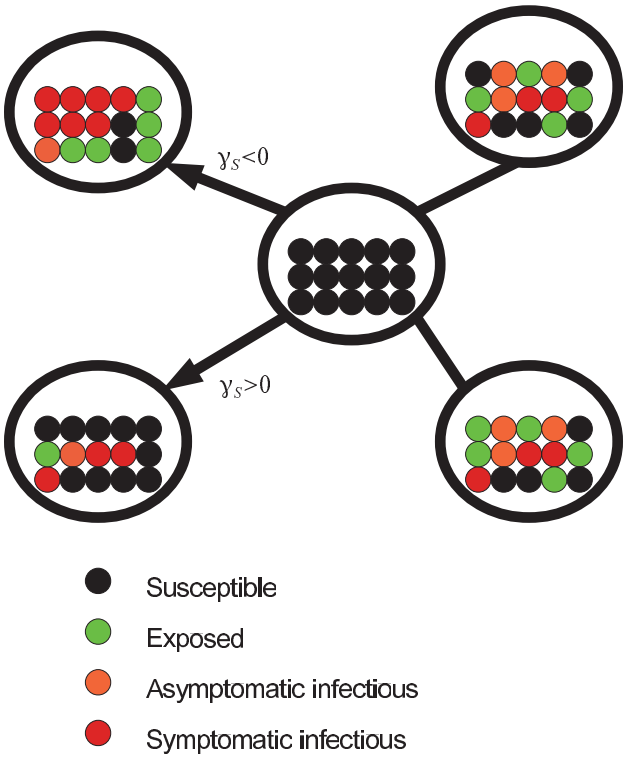

Figure 1 | Schematic illustration of mobility patterns in an SEIS-like model based on a metapopulation approach. There are four states in this model: susceptible (S), exposed (E), asymptomatic infectious (A), and symptomatic infectious (I). The probability that individuals travel to a neighboring city depends on the city's safety level, which is proportional to the average number of susceptible individuals contained in it. γ_S is used to describe the dependency on a city's safety level. For instance, if $\gamma_S > 0$, then susceptible individuals prefer to pass safer cities (safe moves); if $\gamma_S < 0$, then susceptible individuals prefer to bypass safer cities (unsafe moves), that is, the safer a city, the lower is the probability that susceptible individuals travel to it.

where $p(k''|k)$ is the conditional probability that a vertex of degree k connects with a vertex of degree k''. $\Theta_{kk'}^{\sigma}$ represents the fraction of susceptible individuals in subpopulation k' to those around k. If there are no susceptible individuals or even no individuals around subpopulation k, individuals within k randomly travel to one of the neighboring subpopulations; see Methods for details.

Invasion threshold. A key parameter for the description of the spread rate of a disease is represented by the basic reproduction number R_0, which can be analyzed according to the stability of the disease-free equilibrium (DFE)[38]. If $R_0 < 1$, then DFE is locally asymptotically stable, and the disease cannot invade the population; if $R_0 > 1$, then DFE is unstable and invasion is possible. The equilibrium of the model is $\{\rho_{S,k}, \rho_{E,k}, \rho_{A,k}, \rho_{I,k}\} = \{\rho_{S,k}^*, 0, 0, 0\}$ with the constraint $\sum_k p(k)\rho_{S,k}^* = \rho_0$, where ρ_0 is the average density of the population in the network and $p(k)$ is the degree distribution. $\rho_{S,k}^*$ is given by

$$\rho_{S,k}^* = \frac{k\rho_S^*\left(\rho_{S,k}^*\right)^{\gamma_S}}{\sum_{k'} k'p(k')\left(\rho_{S,k'}^*\right)^{\gamma_S}} = \frac{k\rho_0\left(\rho_{S,k}^*\right)^{\gamma_S}}{\left\langle\left(\rho_S^*\right)^{1,\gamma_S}\right\rangle}, \qquad (2)$$

where $\left\langle\left(\rho_S^*\right)^{\cdot,\gamma_S}\right\rangle$ denotes an arbitrary order moment of $\left(\rho_S^*\right)^{\gamma_S}$. The stable solution $\rho_{S,k}^*$ can be solved numerically by using Eq. (2). In particular, if $\gamma_S = 0$, then $\rho_{S,k}^* = \frac{k}{\langle k\rangle}\rho_0$, which means that the higher a

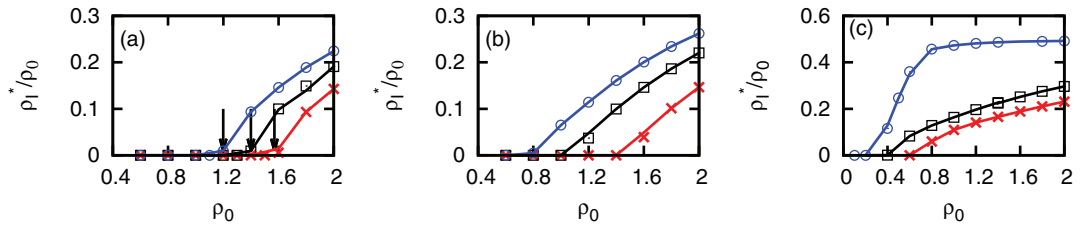

Figure 2 | Prevalence of infected individuals after transient for different kinds of human mobility patterns. (a) $\gamma_S = -1$; (b) $\gamma_S = 0$; (c) $\gamma_S = 1$. Mean-field results (solid lines) and agent-based computer simulations with $\gamma_I = -1$ (crosses), $\gamma_I = 0$ (squares), and $\gamma_I = 1$ (circles). The critical population density depends on human mobility patterns. Arrows in (a) indicate the critical population density predicted using Eq. (3). The mobility rates are set as $D_S = D_E = D_A = D_I = 1$. The degree distribution is $p(k) \sim k^{-3}$ with the network size $N = 2000$, the minimal degree $k_{min} = 2$, and the maximal degree $k_{max} = 44$. Initially, 5% of the population is infectious, and each point is the average result among at least 200 random initial conditions over more than 10 networks.

city's degree k, the greater is the number of individuals that are located in that city.

R_0 can be calculated by the spectral radius of the next-generation matrix, that is, $R_0 = \rho(\mathbf{FV}^{-1})$, where $\rho(\boldsymbol{A})$ denotes the spectral radius of matrix $\boldsymbol{A}$[38]. Let $\mathbf{F}$ denote the matrix of new infections and $\mathbf{V}$ denote the transfer matrix of entering and leaving the compartment. Then $R_0 = \rho(\mathbf{FV}^{-1})$ is given by

$$R_0 = \rho\left(\mathbf{FV}^{-1}\right) = \rho\left(\mathbf{F_A}\mathbf{J_A}^{-1}\mathbf{J_p}\mathbf{J_E}^{-1} + \mathbf{F_I}\mathbf{J_I}^{-1}\mathbf{J_{p'}}\mathbf{J_E}^{-1}\right) = \rho(\mathbf{Q}_1 + \mathbf{Q}_2), \quad (3)$$

which is expected to be the sum of individuals infected by asymptomatic and symptomatic infectious individuals. $\mathbf{F_A}$ (or $\mathbf{F_I}$) is a diagonal matrix with the kth diagonal element equal to $\beta_A \rho^*_{S,k}$ (or $\beta_I \rho^*_{S,k}$). $\mathbf{J_E}$, $\mathbf{J_A}$, $\mathbf{J_I}$, $\mathbf{J_p}$, and $\mathbf{J_{p'}}$ are given by

$$\begin{aligned}
\mathbf{J_E} &= (\epsilon + D_E)\mathbf{I_d} - D_E\mathbf{C_E},\\
\mathbf{J_A} &= (\mu + D_A)\mathbf{I_d} - D_A\mathbf{C_A},\\
\mathbf{J_I} &= (\mu + D_I)\mathbf{I_d} - D_I\mathbf{C_I},\\
\mathbf{J_p} &= \epsilon p_a \mathbf{I_d},\\
\mathbf{J_{p'}} &= \epsilon(1 - p_a)\mathbf{I_d},
\end{aligned} \quad (4)$$

where $\mathbf{I_d}$ is the identity matrix and $\mathbf{C}_\sigma$ ($\sigma = E, A, I$) is the mobility-probability-related matrix for individuals in state σ given by

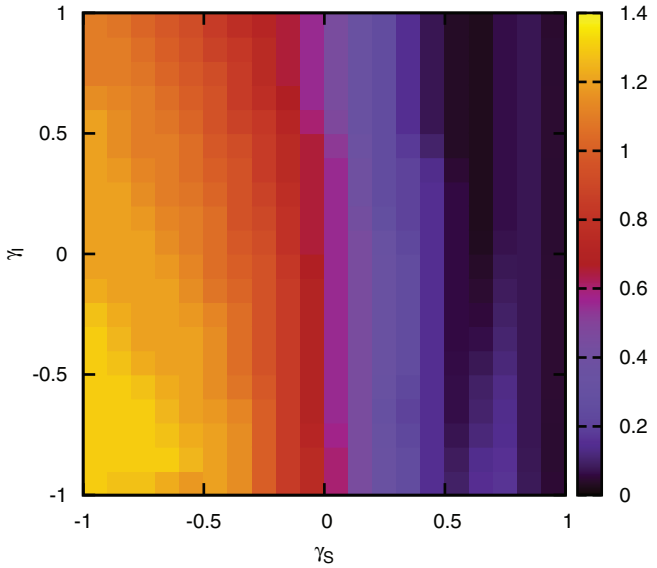

Figure 3 | Dependence of the critical population density on γ_S and γ_I. The color indicates the value of the critical population density ρ_{0c} in networks with $N = 2000$, $k_{min} = 2$, and $k_{max} = 44$. The degree distribution is $p(k) \sim k^{-3}$. The mobility rates are set as $D_S = D_E = D_A = D_I = 1$.

$$\mathbf{C}_{\sigma,ij} = ip(j|i)\Theta^\sigma_{ji} = \frac{ijp(j)}{\langle k\rangle}\Theta^\sigma_{ji}, \quad \text{for } \sigma = E, A, I, \text{ and } i, j = k_{min}, \ldots, k_{max}, \quad (5)$$

where the minimal degree is denoted by k_{min} and the maximal degree is denoted by k_{max}. Obviously, $\mathbf{C}_\sigma$ is a rank-one matrix, and hence, it can be expressed in the form $\mathbf{C}_\sigma = \omega_\sigma v^T$, where ω_σ and v are column vectors with $\omega_{\sigma,i} = i\Theta^\sigma_{1i}$ and $v_j = \dfrac{p(j)}{\langle k\rangle}$.

The two terms on the right-hand side in Eq. (3) are further expressed as

$$\begin{aligned}
\mathbf{Q}_1 &= diag(a_k)\left(\mathbf{I_d} + vv^T\right),\\
\mathbf{Q}_2 &= diag(b_k)\left(\mathbf{I_d} + \mu v^T\right),
\end{aligned} \quad (6)$$

where coefficients $a_k = \dfrac{\beta_A \rho^*_{S,k}\epsilon p_a}{(\mu + D_A)(\epsilon + D_E)}$ and $b_k = \dfrac{\beta_I \rho^*_{S,k}\epsilon(1 - p_a)}{(\mu + D_I)(\epsilon + D_E)}$. The two column vectors v and μ are expressed as $v = c_A\omega_A + c_E\omega_E + c_Ac_E\omega_A v^T\omega_E$ and $\mu = c_I\omega_I + c_E\omega_E + c_Ic_E\omega_I v^T\omega_E$, where coefficients $c_A = \dfrac{1}{1 - \dfrac{D_A}{\mu + D_A}\sum_k C_{A,kk}} \cdot \dfrac{D_A}{\mu + D_A}$, $c_I = \dfrac{1}{1 - \dfrac{D_I}{\mu + D_I}\sum_k C_{I,kk}} \cdot \dfrac{D_I}{\mu + D_I}$, and $c_E = \dfrac{1}{1 - \dfrac{D_E}{\epsilon + D_E}\sum_k C_{E,kk}} \cdot \dfrac{D_E}{\epsilon + D_E}$ (see Supplementary Information for details). Thus, the eigenvalue λ of the matrix $\mathbf{Q_1} + \mathbf{Q_2}$ can be solved using the secular equation[39] as follows:

$$1 + \sum_k \frac{v_k(a_kv_k + b_k\mu_k)}{d_k - \lambda} = 0, \quad (7)$$

where $d_k = a_k + b_k$. In the case of random mobility when $\gamma_\sigma = 0$, $\sum_k \mathbf{C}_{\sigma,kk} = 1$, and the critical invasion threshold does not change with human behavior. However, if $\gamma_\sigma \neq 0$, then human behavior affects the invasion threshold by influencing c_σ, which is a function of $\sum_k \mathbf{C}_{\sigma,kk}$. Therefore, for the equilibrium to be unstable, the maximal eigenvalue λ_{max} in Eq. (7) should be greater than 1.

Therefore, the threshold condition of the critical population density ρ_{0c} is extremely relevant to individuals' mobility patterns responding to the safety information, with which we can understand how these patterns affect the epidemic behavior.

Human behavior in configuration network models. To explore how safety-information-driven human mobility patterns influence the spread of an infectious disease, we performed a number of agent-based simulations with the configuration network models. For nonlimited infection, there exists a critical population density ρ_{0c} that allows a disease to invade the population (see Supplementary Information). The phase transitions of the model with different kinds of human behavior are shown in Fig. 2, which indicates that the

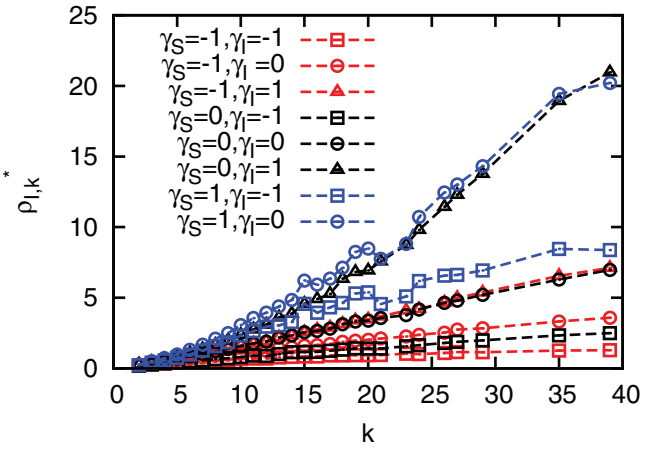

Figure 4 | Average number of infected individuals at subpopulation *k* for different kinds of mobility patterns. The population density is fixed at $\rho_0 = 2$ and other parameters are the same as in Fig. 2.

invasion threshold ρ_{0c} alters with human mobility patterns. In addition, if infectious individuals take unsafe moves when $\gamma_I < 0$ (the red curve in each panel), then the separation of infectious and susceptible individuals prevents the spread of the disease with an increased invasion threshold ρ_{0c} and a decreased outbreak size. This achieves best when both susceptible individuals and infected individuals take unsafe moves ($\gamma_S = \gamma_I = -1$ in Fig. 2 (a)), which can cause only a very limited size of infection, and thus, cities that are highly populated with susceptible individuals are protected from infection. However, if all infectious individuals prefer safe moves when $\gamma_I > 0$ (the blue curves in Fig. 2), then the increased contact rates between infectious and susceptible individuals facilitate the spread of an infectious disease with a dramatically decreased ρ_{0c} and an increased outbreak size. This situation worsens further if susceptible individuals also execute safer moves ($\gamma_S = \gamma_I = 1$, see Fig. 2(c)). The result demonstrates the importance of protecting highly populated cities that are not yet infected and the crucial role of human mobility patterns in the epidemic behavior. In details, while safe moves decrease the individual's risk of being infected, this behavior unexpectedly increases the risk of infection via the entire network with a huge outbreak. On the contrary, while unsafe moves increase the individual's risk of being infected, this behavior efficiently protects the main network and prevents the disease spread with a relatively small outbreak size. The dependence of the critical population density on human behavior is shown in Fig. 3, indicating that the critical population density decreases as γ_S (or γ_I) increases.

Distribution of infected individuals in the networks. To understand the origin of various outbreak sizes under different human mobility patterns, we investigate the distribution of infected individuals in the network by estimating the average numbers of infected individuals after transition in each subpopulation *k*, as shown in Fig. 4. It is observed that the number of infected individuals at each vertex increases with the degree in an approximately linear manner, indicating that the larger a vertex degree, the higher is the number of contained infected individuals. This effect is dramatically enhanced when individuals execute safer moves to highly populated areas (with an increase in γ_S or γ_I) because the gathering of individuals at hub-like vertices increases the contact rates between susceptible and infectious individuals. When individuals take unsafe moves, this behavior can efficiently avoid the gathering of individuals at hub vertices, as a result, the number of infected individuals at hub-like vertices is only slightly increased. Therefore, unsafe moves efficiently protect the individuals at high degree vertices from infection and thus suspend the spread of the disease. This suggests the importance of protecting hub-like vertices during the outbreak of an infectious disease. The role of unsafe moves

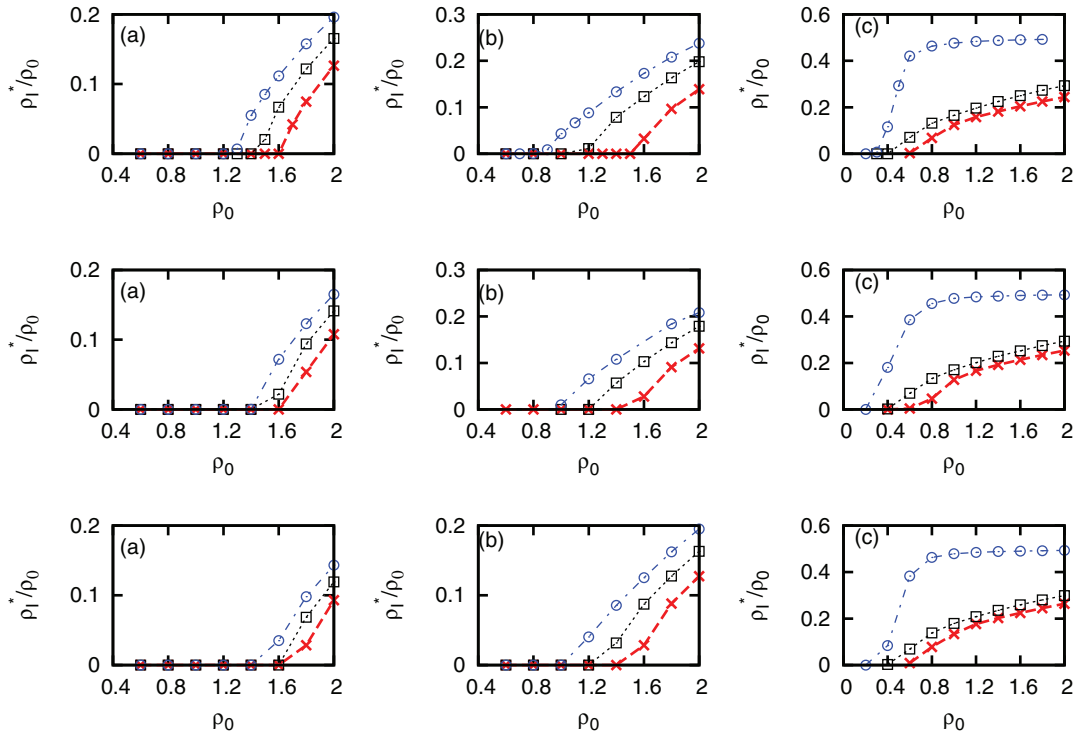

Figure 5 | Comparison of the efficiencies of travel restrictions on symptomatic infectious individuals. $D_I = 0.5$ (top); $D_I = 0.2$ (middle); and $D_I = 0.0$ (bottom). Individuals in other states are free to move with $D_S = D_E = D_A = 1$. (a) $\gamma_S = -1$; (b) $\gamma_S = 0$; (c) $\gamma_S = 1$. In each panel, $\gamma_I = -1$ (crosses), $\gamma_I = 0$ (squares), and $\gamma_I = 1$ (circles). Other parameters are the same as in Fig. 2.

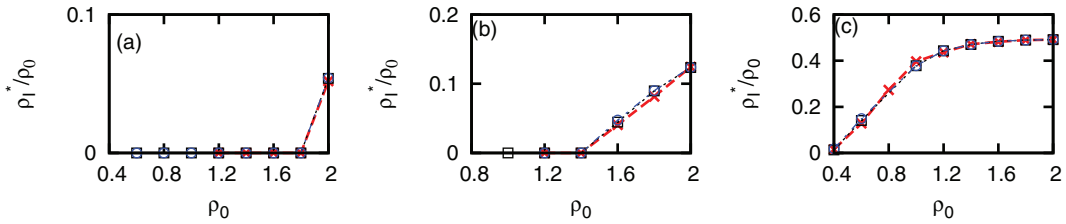

Figure 6 | Comparison of the efficiencies of travel restrictions on both symptomatic and asymptomatic infectious individuals with different kinds of human mobility patterns. D_A and D_I are set to be zero and individuals in other states are free to move with $D_S = D_E = 1$. (a) $\gamma_S = -1$; (b) $\gamma_S = 0$; (c) $\gamma_S = 1$. In each panel, $\gamma_I = -1$ (crosses), $\gamma_I = 0$ (squares), and $\gamma_I = 1$ (circles). Other parameters are the same as in Fig. 2.

is similar to the control measure, such as dispersing people at hub-like vertices into different areas, which would help suspend the outbreak of an infectious disease, as when we were warned not to go to the public places during the outbreak of SARS[40].

The role of hub-like vertices also allows us to expect that more individuals would gather there due to the effect of heterogeneous network structure, as observed in other mobility patterns such as random ($\gamma_S = \gamma_I = 0$) or traffic dependent mobility patterns[8] and safe (unsafe) moves would strengthen (weaken) this effect.

Efficacy of travel restrictions. To understand the effectiveness of a control strategy such as travel restrictions in the event of the outbreak of an infectious disease, travel restrictions imposed on symptomatic infectious individuals under different human mobility patterns are implemented, as shown in Fig. 5. The mobility rate is gradually decreased from $D_I = 0.5$ (top) and $D_I = 0.2$ (middle) to $D_I = 0.0$ (bottom) (Fig. 5). However, no significant reduction in the outbreak size is observed by implementing this measure for different mobility patterns ($D_I = 0.5$ and 0.2 in the top and middle, respectively, in Fig. 5), even when an absolute travel restriction with $D_I = 0$ is imposed (bottom in Fig. 5). The relative reduction in the prevalence of infected individuals is less than 36% for all mobility patterns. The inefficiency of travel restrictions to reduce the outbreak is consistent with the observation in Ref. 36, and it has been explained by the heterogeneity in network topology. However, in the present framework, travel restrictions could prevent the disease spread under some conditions, for example, constraining the movements of symptomatic infectious individuals who take safe moves (the blue curves in the first column in Fig. 5); this effect becomes weak when susceptible individuals also take safe moves (the second and third columns in Fig. 5). The result suggests that the efficiency of travel restrictions imposed on symptomatic infectious individuals depends not only on their own mobility patterns but also on susceptible individuals' mobility patterns.

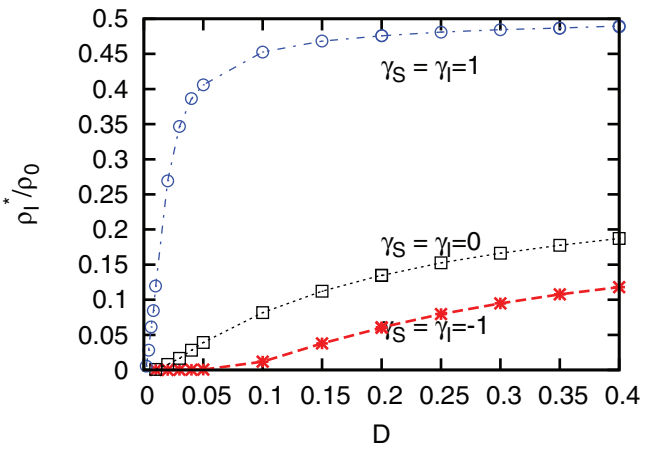

Figure 7 | Prevalence of infected individuals after transient versus the mobility rate D for different kinds of human mobility patterns. The mobility rates for all individuals are assumed to be same with $D_S = D_E = D_A = D_I = 1$. The population density is fixed at $\rho_0 = 2$. Other parameters are the same as in Fig. 2.

Then, we anticipate the high efficiency of travel restrictions for both symptomatic and asymptomatic infectious individuals. Figure 6 shows again that the efficiency of this control measure is strictly dependent on the mobility patterns of susceptible individuals. For instance, if susceptible individuals take unsafe moves, the outbreak size is dramatically reduced (Fig. 6 (a)); otherwise, as compared with Fig. 2, there is no obvious improvement in outbreak sizes (Figs. 6 (b) and (c)). Therefore, it shows again the crucial effect of susceptible individuals' mobility patterns on the efficiency of travel restrictions on infectious individuals.

Effects of mobility patterns on critical mobility rate. As for the effects of human mobility patterns on the critical mobility rate, we assume that individuals in all states travel at the same rate, that is, $D_S = D_E = D_A = D_I = D$. Figure 7 shows the prevalence of infected individuals at the end of a global epidemic as a function of the mobility rate D. The critical mobility rate D depends on how individuals respond to the safety information. For instance, as compared with the null model ($\gamma_S = \gamma_I = 0$), safe moves promote the spread of a disease with a reduced critical mobility rate and an increased outbreak size, which further confirms that personal consideration of escaping infection facilitates the disease spread to the entire network, while unsafe moves counterintuitively suspend the spread of a disease.

Human mobility in the Japanese domestic airline network. To obtain more realistic results and to further confirm the validity of the model, we subsequently examined the concept of safety-information-driven human mobility as applied to the Japanese domestic airline network in Fig. 8. While incorporating practical data into the model would be more realistic, due to the difficulty of obtaining the data, the mobility rate and the dependence on the safety information are assumed constant. We then turn our focus to modeling safety-information-driven mobility patterns in real world network structure. The data of the Japanese domestic airline network were obtained from the websites of the Haneda and Narita airports, from which a list of direct flights to other airports was obtained, and subsequently each flight was iteratively tracked. A network in which each vertex represents an airport and each link denotes a direct flight between two airports was constructed. The prevalence of infected individuals after transient for different mobility patterns are shown in Figs. 9 and 10, which qualitatively agree with the previous results obtained from the configuration network model.

From the above analysis, we can deduce that human responses to safety information substantially affect the epidemic behavior in such a way that personal consideration of safe moves eventually causes a huge outbreak in the entire network, while unsafe moves may protect the network from infection. Moreover, the efficiency of travel

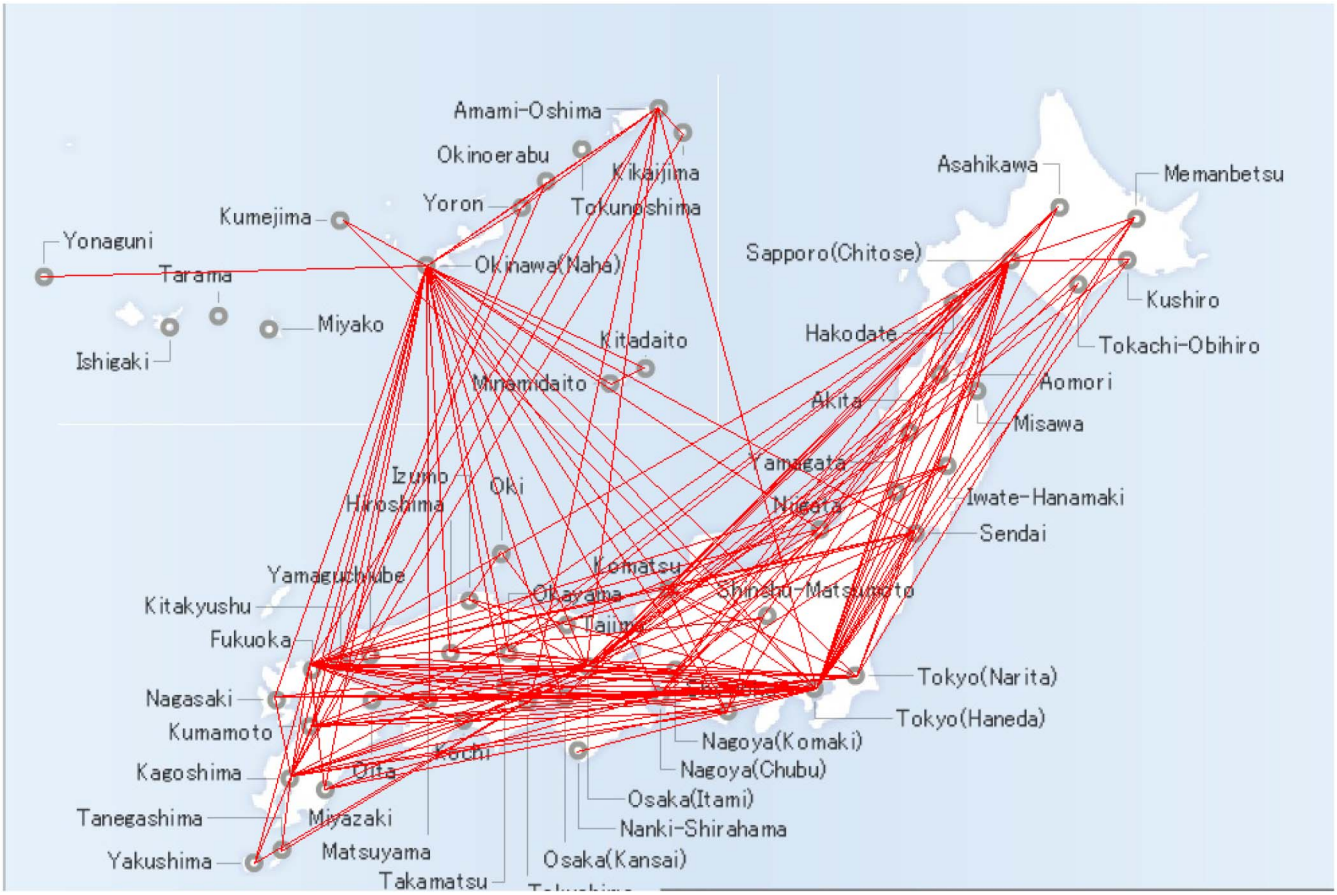

Figure 8 | Japanese domestic airline network. Fifty main airports in the Japanese domestic airline network are connected. The total number of airports is $N = 79$, and the average degree is $\langle k \rangle = 6$. The maximal degree $k_{max} = 55$ corresponds to Tokyo (Haneda), and other hub-like airports include Osaka (Kansai), which is in the center of west Japan, and Okinawa (Naha), which is a representative tourist resort. This figure was modified from the route map of Japan Airlines (http://www.jal.co.jp/en/dom_network).

restrictions on symptomatic individuals closely relates with healthy individuals' mobility patterns (see the Supplementary Information).

Discussion

Although much work has been done on human mobility patterns in daily lives such as recurrent mobility with a memory (i.e., commuting)[27] and a complex global airline transportation network[24], the study of mobility driven by safety consideration is still an important open problem. As a first attempt to capture this factor, we have assumed that human mobility to a city is solely dependent upon the city's safety level. To avoid exposure to the disease, individuals typically execute safe moves, but unfortunately, this personal consideration facilitates the global spread of the disease with an increased outbreak size and a small critical threshold.

Note that the safety-information-driven mobility to a city strongly depends on how a city's safety level is defined. We have considered that a city's safety level is proportional to its healthy population size or the number of healthy people. As an alternative, it is also reasonable to assume that a city's safety level is proportional to its healthy population density, that is, the density of susceptible individuals in it in the form of $\frac{\rho_{S,k}}{\rho_k}$. In this case, the critical population density is independent of human mobility patterns and does not change with them (see the Supplementary Information). Our analysis also explains the result of a related work[41] that the invasion threshold does not vary with human behavior, where based on the susceptible-infected-removed (SIR) model, the mobility probability to a city is proportional to the total density of healthy people and

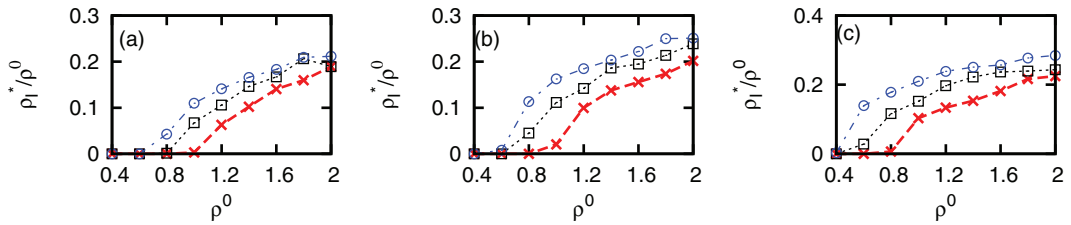

Figure 9 | Prevalence of infected individuals after transient with different kinds of human mobility patterns in the Japanese domestic airline network. (a) $\gamma_S = -1$; (b) $\gamma_S = 0$; (c) $\gamma_S = 1$. In each panel, $\gamma_I = -1$ (crosses), $\gamma_I = 0$ (squares), and $\gamma_I = 1$ (circles). The mobility rates are set as $D_A = D_E = D_A = D_I = 1$. Initially, one infectious seed is introduced in the network. Each point is the average of 500 random initial conditions. Other parameters are the same as in Fig. 2.

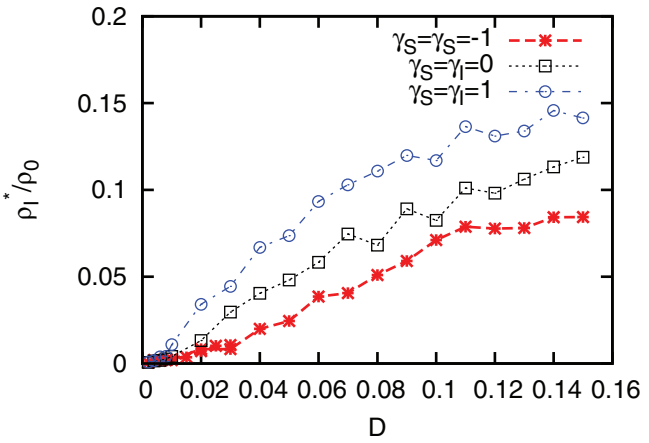

Figure 10 | Prevalence of infected individuals after transient versus *D* for different kinds of human mobility patterns in the Japanese domestic airline network. The population density is fixed at $\rho_0 = 2$, and $D_S = D_E = D_A = D_I = D$. Other parameters are the same as in Fig. 2.

removed people in that city. Therefore, the definition of a city's safety level has important consequences on the epidemic behavior.

Given the importance of spatial spread of human infectious diseases, this study demonstrates the crucial role played by human mobility in the epidemic spreading process. According to our results, on one hand, although personal consideration of safe moves decreases the individual's risk of being infected, this behavior unexpectedly increases the risk of outbreak in the entire network; on the other hand, while unsafe moves increase the individual's risk of being infected, this behavior protects the main network from serious infection. Despite the encouraging results, it should be noted that our conclusion solely holds under the present situation, and a more realistic situation incorporating the factor of recurrent mobility[27] or traveling[37] would enrich our model and deserve further consideration. Even so, the present study is relevant to a kind of a benefit-driven mobility model, where individuals optimize their moves to the safest neighboring destination in order to maximize their own benefits or minimize their risk of infection, and conversely this mobility scheme affects the epidemic prevalence of the entire network. This corresponds to an extreme case of our model with a determinate choice of mobility destination and similar results to the condition with $\gamma > 0$ would be expected. Further discussion of coevolution dynamics within behavioral epidemiology and sociology would help us better understand the spatial spread of an infectious disease in social networks. We hope that our result would stimulate further work in this direction.

Methods

Model structure. Differently from the individual-based model, where a detailed contact network among individuals is characterized[42–46], metapopulation structured models consider the system divided into connected subpopulations along which individuals travel via transportation. Inside each subpopulation, homogeneous mixing is often assumed, with which mathematical modeling is able to capture the travel flows among subpopulations[23,31,32,36]. A detailed comparison of the two models is beyond the present study but can be found in Ref. 46. At the metapopulation level, in each subpopulation with degree k, the epidemic process is assumed to be an all-to-all interaction at rate $\beta_I \rho_{S,k} \rho_{I,k}$ or $\beta_A \rho_{S,k} \rho_{A,k}$, where $\rho_{S,k}$, $\rho_{I,k}$, and $\rho_{A,k}$ are the average numbers of susceptible, symptomatic, and asymptomatic infectious individuals, respectively. With the continuous-time formulation of the disease spread in metapopulation models and the assumption of nonlimited transmission, the mean-field approximation governing the dynamics of a disease spread in subpopulation $k \in [k_{min}, k_{max}]$ is given by

$$\frac{d\rho_{S,k}}{dt} = \mu(\rho_{A,k} + \rho_{I,k}) - \rho_{S,k}(\beta_A \rho_{A,k} + \beta_I \rho_{I,k}) - D_S \rho_{S,k} + k \sum_{k'} p(k'|k) \rho_{S,k'} \Theta^S_{k'k} D_S, \quad (8)$$

$$\frac{d\rho_{E,k}}{dt} = -\epsilon \rho_{E,k} + \rho_{S,k}(\beta_A \rho_{A,k} + \beta_I \rho_{I,k}) - D_E \rho_{E,k} + k \sum_{k'} p(k'|k) \rho_{E,k'} \Theta^E_{k'k} D_E, \quad (9)$$

$$\frac{d\rho_{A,k}}{dt} = -\mu \rho_{A,k} + \epsilon p_a \rho_{E,k} - D_A \rho_{A,k} + k \sum_{k'} p(k'|k) \rho_{A,k'} \Theta^A_{k'k} D_A, \quad (10)$$

$$\frac{d\rho_{I,k}}{dt} = -\mu \rho_{I,k} + \epsilon(1 - p_a) \rho_{E,k} - D_I \rho_{I,k} + k \sum_{k'} p(k'|k) \rho_{I,k'} \Theta^I_{k'k} D_I, \quad (11)$$

where k_{min} and k_{max} are the minimal and maximal degrees, respectively; $p(k'|k)$ is the conditional probability that a vertex of degree k connects with a vertex of degree k'. In uncorrelated networks, $p(k'|k) = \frac{k' p(k')}{\langle k \rangle}$, where $\langle k \rangle = \sum_k k p(k)$ is the average connectivity of the network[47]. $\Theta^\sigma_{k'k}(\sigma = S,E,A,I)$ is the probability that individuals in state σ travel from subpopulation k' to a neighboring subpopulation k.

Configuration network models. The substrate networks are generated by the configuration model based on the Molloy-Reed algorithm[48]. Each vertex i is assigned a degree k_i from a given degree distribution $p(k) \sim k^{-\alpha}$ ($\alpha > 2$), which is subject to the restriction $k_i < N^{\frac{1}{2}}$ to avoid the degree correlation, where N is the network size. Sensitivity analyses were implemented on networks generated with the configuration network model with different degree exponents $\alpha = 2.5$ and $\alpha = 3.5$ (see the Supplement Information) as well as Erdős-Rényi networks, and we obtained similar results. For simplicity, we assume throughout the study that exposed individuals behave like susceptible individuals when $\gamma_E = \gamma_S$; analogously, asymptomatic individuals behave like symptomatic individuals when $\gamma_A = \gamma_I$. Further, in this paper, we use the epidemiological parameters $\mu = 0.5$, $\epsilon = 1$, $p_a = 0.5$, and $2\beta_A = \beta_I = 0.5$.

1. Watts, D. J., Muhamad, R., Medina, D. C. & Dodds, P. S. Multiscale, resurgent epidemics in a hierarchical metapopulation model. *Proc. Natl. Acad. Sci. USA* **102**, 11157–11162 (2005).
2. Colizza, V., Barrat, A., Barthélemy, M. & Vespignani, A. The role of the airline transportation network in the prediction and predictability of global epidemics. *Proc. Natl. Acad. Sci. USA* **103**, 2015–2020 (2006).
3. Camitz, M. & Liljeros, F. The effect of travel restrictions on the spread of a moderately contagious disease. *BMC Med.* **4**, 32 (2006).
4. Colizza, V., Pastor-Satorras, R. & Vespignani, A. Reaction-diffusion processes and metapopulation models in heterogeneous networks. *Nature Phys.* **3**, 276–282 (2007).
5. Colizza, V. & Vespignani, A. Invasion threshold in heterogeneous metapopulation networks. *Phys, Rev. Lett.* **99**, 148701 (2007).
6. Vazquez, A. Epidemic outbreaks on structured populations. *J. Theor. Biol.* **245**, 125–129 (2007).
7. Colizza, V., Barrat, A., Barthélemy, M., Valleron, A.-J. & Vespignani, A. Modeling the worldwide spread of pandemic influenza: baseline case and containment interventions. *PLoS Med.* **4**, e13 (2007).
8. Colizza, V. & Vespignani, A. Epidemic modeling in metapopulation systems with heterogeneous coupling pattern: theory and simulations. *J. Theor. Biol.* **251**, 450–467 (2008).

9. Saldaña, J. Continuous-time formulation of reaction-diffusion processes on heterogeneous metapopulations. *Phys. Rev. E* **78**, 012902 (2008).
10. González, M. C., Hidalgo, C. A. & Barabási, A.-L. Understanding individual human mobility patterns. *Nature* **453**, 779–782 (2008).
11. Gross, T., D'Lima, C. J. D. & Blasius, B. Epidemic dynamics on an adaptive network. *Phys. Rev. Lett.* **96**, 208701 (2006).
12. Gross, T. & Blasius, B. Adaptive coevolutionary networks: a review. *J. R. Soc. Interface* **5**, 259–271 (2008).
13. Juher, D., Ripoll, J. & Saldaña, J. Analysis and Monte Carlo simulations of a model for the spread of infectious diseases in heterogeneous metapopulations. *Phys. Rev. E* **80**, 041920 (2009).
14. Meloni, S., Arenas, A. & Moreno, Y. Traffic-driven epidemic spreading in finite-size scale-free networks. *Proc. Natl. Acad. Sci. USA* **106**, 16897–16902 (2009).
15. Wang, P., González, M. C., Hidalgo, C. & Barabási, A.-L. Understanding the spreading patterns of mobile phone viruses. *Science* **324**, 1071 (2009).
16. Wang, B., Aihara, K. & Kim, B. J. Comparison of immunization strategies in geographical networks. *Phys. Lett. A* **373**, 3877–3882 (2009).
17. Barthélemy, M., Godreche, C. & Luck, J.-M. Fluctuation effects in metapopulation models: percolation and pandemic threshold. *J. Theor. Biol.* **267**, 554–564 (2010).
18. Masuda, N. Effects of diffusion rates on epidemics spreads in metapopulation networks. *New J. Phys.* **12**, 093009 (2010).
19. Funk, S., Salathé, M. & Jansen, V. A. A. Modelling the influence of human behavior on the spread of infectious diseases: a review. *J. Roy. Soc. Interface* **7**, 1247–1256 (2010).
20. Keeling, M. J., Danon, L., Vernon, M. C. & House, T. A. Individual identity and movement networks for disease metapopulations. *Proc. Natl. Acad. Sci. USA* **107**, 8866–8870 (2010).
21. Cao, L., Li, X., Wang, B. & Aihara, K. Rendezvous effects in the diffusion process on bipartite metapopulation networks. *Phys. Rev. E* **84**, 041936 (2011).
22. Balcan, D. *et al.* Multiscale mobility networks and the spatial spreading of infectious diseases. *Proc. Natl. Acad. Sci. USA* **106**, 21484–21489 (2009).
23. Balcan, D. *et al.* Modeling the spatial spread of infectious diseases: the global epidemic and mobility computational model. *J. Comput. Sci.* **1**, 132–145 (2010).
24. Barrat, A., Barthélemy, M., Pastor-Satorras, R. & Vespignani, A. The architecture of complex weighted networks. *Proc. Natl. Acad. Sci. USA* **101**, 3747–3752 (2004).
25. Brockmann, D., Hufnagei, L. & Geisel, T. The scaling laws of human travel. *Nature* **439**, 462–465 (2006).
26. Brockmann, D. & Theis, F. Money circulation, trackable items, and the emergence of universal human mobility patterns. *IEEE Pervasive Comput.* **7**, 28–35 (2008).
27. Balcan, D. & Vespignani, A. Phase transitions in contagion processes mediated by recurrent mobility patterns. *Nature Phys.* **7**, 581–586 (2011).
28. Song, C., Qu, Z., Blumm, N. & Barabási, A.-L. Limits of predictability in human mobility. *Science* **327**, 1018–1021 (2010).
29. Song, C., Koren, T., Wang, P. & Barabási, A.-L. Modelling the scaling properties of human mobility. *Nature Phys.* **6**, 818–823 (2010).
30. Balcan, D. & Vespignani, A. Invasion threshold in structured populations with recurrent mobility patterns. *J. Theor. Biol.* **293**, 87–100 (2012).
31. Belik, V., Geisel, T. & Brockmann, D. Natural human mobility patterns and spatial spread of infectious diseases. *Phys. Rev. X* **1**, 011001 (2011).
32. Belik, V., Geisel, T. & Brockmann, D. Recurrent host mobility in spatial epidemics: beyond reaction-diffusion. *Eur. Phys. J. B* **84**, 579–587 (2011).
33. Vespignani, A. Modelling dynamical processes in complex socio-technical systems. *Nature Phys.* **8**, 32–39 (2012).
34. Bagrow, J. P., Wang, D. & Barabási, A.-L. Collective response of human populations to large-scale emergencies. *PLoS ONE* **6**, e17680 (2011).
35. Funk, S., Gilad, E., Watkins, C. & Jansen, V. A. A. The spread of awareness and its impact on epidemic outbreaks. *Proc. Natl. Acad. Sci. USA* **106**, 6872–6877 (2009).
36. Bajardi, P. *et al.* Human mobility networks, travel restrictions, and the global spread of 2009 H1N1 pandemic. *PLoS ONE* **6**, e16591 (2011).
37. Poletto, C., Tizzoni, M. & Colizza, V. Heterogeneous length of stay of hosts' movements and spatial epidemic spread. *Sci. Rep.* **2**, 476 (2012).
38. van den Driessche, P. & Watmough, J. Reproduction numbers and sub-threshold endemic equilibria for compartmental models of disease transmission. *Math. Biosci.* **180**, 29–48 (2002).
39. Anderson, J. A secular equation for the eigenvalues of a diagonal matrix perturbation. *Linear Algebra Appl.* **246**, 49–70 (1996).
40. Deurenberg-Yap, M. *et al.* The Singaporean response to the SARS outbreak: knowledge sufficiency versus public trust. *Health Promot. Int.* **20**, 320–326 (2005).
41. Meloni, S. *et al.* Modeling human mobility responses to the large-scale spreading of infectious disease. *Sci. Rep.* **1**, 62 (2011).
42. Liljeros, F., Edling, C. R., Amaral, L. A. N., Stanley, H. E. & Aberg, Y. The web of human sexual contacts. *Nature* **411**, 907–908 (2001).
43. Liljeros, F., Giesecke, J. & Holme, P. The contact network of inpatients in a regional healthcare system. A longitudinal case study. *Math. Popul. Stud.* **14**, 269–284 (2007).
44. Stehlé, J. *et al.* Simulation of an SEIR infectious disease model on the dynamic contact network of conference attendees. *BMC Med.* **9**, 87 (2011).
45. Balcan, D. *et al.* Seasonal transmission potential and activity peaks of the new influenza a (H1N1): a Monte Carlo Likelihood analysis based on human mobility. *BMC Med.* **7**, 45 (2009).
46. Ajelli, M. *et al.* Comparing large-scale computational approaches to epidemic modeling: agent-based versus structured metapopulation models. *BMC Infect. Dis.* **10**, 190 (2010).
47. Newman, M. E. J. Mixing patterns in networks. *Phys. Rev. E* **67**, 026126 (2003).
48. Molloy, M. & Reed, B. A critical point for random graphs with a given degree sequence. *Random Struct. Algor.* **6**, 161–179 (1995).

Acknowledgments

This research is supported by the "Funding Program for World-Leading Innovative *R&D* on Science and Technology (FIRST Program)" initiated by the Council for Science and Technology Policy (CSTP) (B.W., H.S., and K.A.), as well as by the Japan Science and Technology Agency (JST) "Precursory Research for Embryonic Science and Technology (PRESTO) program" (H.S.).

Author contributions

BW, LC, HS, and KA planned the study; BW and LC performed the experiments, analyzed the data, and prepared the figures; BW, LC, HS, and KA wrote the paper.

Additional information

Supplementary information accompanies this paper at http://www.nature.com/scientificreports

Competing financial interests: The authors declare no competing financial interests.

How to cite this article: Wang, B., Cao, L., Suzuki, H. & Aihara, K. Safety-Information-Driven Human Mobility Patterns with Metapopulation Epidemic Dynamics. *Sci. Rep.* **2**, 887; DOI:10.1038/srep00887 (2012).